

Verification, Validation and Testing of Kinetic Mechanisms of Hydrogen Combustion in Fluid Dynamic Computations

Victor P. Zhukov

Institute of Space Propulsion, German Aerospace Center (DLR), Lampoldshausen, 74239 Hardthausen, Germany. Ph.: +49-(0)6298-28-633, Fax: +49-(0)6298-28-458

Abstract

A one-step, a two-step, an abridged, a skeletal and four detailed kinetic schemes of hydrogen oxidation have been tested. A new skeletal kinetic scheme of hydrogen oxidation has been developed. The CFD calculations were carried out using ANSYS CFX software. Ignition delay times and speeds of flames were derived from the computational results. The computational data obtained using ANSYS CFX and CHEMKIN, and experimental data were compared. The precision, reliability, and range of validity of the kinetic schemes in CFD simulations were estimated. The impact of kinetic scheme on the results of computations was discussed. The relationship between grid spacing, timestep, accuracy, and computational cost were analyzed.

Keywords: CFD modelling, chemical kinetics, hydrogen, combustion, flame

Email address: vpzhukov@gmail.com (Victor P. Zhukov)

1. Introduction

In the last decade commercial software packages: ANSYS CFX [1], Fluent [2], Star-CD [3], etc. are widely used as a tool for solving Computational Fluid Dynamics (CFD) problems. According to web site top500.org, computational capabilities are increasing by a factor of 100 every eight years. The explosive growth of computational power allows to carry out CFD simulations using more and more complicated physical models on small clusters of computers or even desktop computers (without using high-power expensive computers). The modern CFD simulations can be multicomponent, multiphase and multidomain. Heat, mass and radiation transfer as well as chemical processes can be taken into account in calculations. The increased amount of model assumptions and parameters is an significant source of errors and faults.

The processes of verification and validation are very important in CFD [4]. They are ground steps in obtaining a numerical solution (Fig. 1). The validation should be done prior to the obtaining of the desired numerical results while the verification should be done prior the validation. Normally, the whole numerical model, which includes equations of fluid dynamics, equation of state and the model of turbulence, is already verified by the developer of the CFD code and the user should verify only its own user defined models. Our ultimate aim is the modeling of the flow in a rocket combustion chamber. In this case we cannot rely on the predefined numerical model, but should use the models which takes into account the specifics of this complicated problem. Here we are focusing on the usage of the chemical kinetic models of hydrogen combustion. In most cases the assumption of thin flame (infinitely

26 fast chemical reactions) gives reliable results, so there is no actual need to use
27 the detailed kinetic mechanisms in CFD simulations. However, the assump-
28 tion of thin flame is not completely satisfied in rocket combustion chamber
29 where the turbulence is very high. By this reason the model of the chemical
30 kinetics should be used for the modeling of the combustion in rocket engine,
31 but before the model should be verified and validated.

32 In our case the verification can be done through the comparison with
33 Chemkin [5] which solves a system of kinetic equations. This gives us a chance
34 to find and eliminate misprints and to prove that numerical parameters, for
35 example time-step and grid, do not determine the solution. The next step
36 should be the validation. After entering into a CFD code a chemical kinetic
37 model became a part of large physical–chemical numerical model. Generally,
38 kinetic mechanisms are already validated extensively by their authors, but
39 after the implementation of the chemical kinetic model the CFD numerical
40 model needs the validation. Of course chemical reactions drive combustion,
41 but indeed combustion processes depend on heat and mass transfer too. Al-
42 though turbulence model, equations of state, transport coefficients, chem-
43 ical kinetic mechanism can be validated separately, the resulting physical–
44 chemical model needs the final validation as a whole.

45 Probably the first example of the verification and the validation of hydro-
46 gen reaction mechanism in CFD simulations is the work by Mani *et al.* [6].
47 A supersonic flow in a constant-area channel was simulated. The employed
48 kinetic scheme consisted of 8 reactions without the kinetics of the peroxides.
49 The supersonic combustion of a hydrogen–air mixture at a high temperat-
50 ure was modeled. The simple kinetic scheme reproduced experimental data

51 properly, what is not surprising when the initial temperature is about 1400
52 K.

53 In 1988 Jachimowski [7] modeled scramjet combustion using of a hydro-
54 gen-air reaction mechanism. He carried out the simulations of hydrogen
55 combustion at parameters related to flight Mach number 8, 16 and 25. The
56 hydrogen-air reaction mechanism consisted of 33 reactions, where the de-
57 tailed hydrogen-oxygen kinetics consisted of 20 reactions. In his study it
58 was shown that chemical kinetics of HO_2 is important at all the studied
59 Mach numbers. Later Eklund and Stouffer [22] carried out the 3-D CFD
60 simulation of a flow in a supersonic combustor. They tested two kinetic
61 models: the detailed model by Jachimowski and the model abridged from
62 the detailed one. This model was obtained by cutting the kinetics of HO_2
63 and H_2O_2 . The new model consists of only 7 reactions within 6 species plus
64 bath gas N_2 . This abridged model is very extensively cited and used due
65 to the low required computational power in the comparison with detailed
66 kinetic models.

67 Kumaran and Babu [8] studied the effect of chemical kinetic models on
68 CFD calculations. They modeled a compressible, turbulent, reacting flow,
69 which simulates the supersonic combustion of hydrogen in the jet engine of
70 hypersonic projectile. The idea of their work is to compare the results ob-
71 tained using the detailed kinetic model with the previous results obtained
72 using a single step kinetics. In their past study they attributed the differ-
73 ence between the numerical results and the experimental data to the inad-
74 equacy of the one-equation turbulence model and the one-step chemistry.
75 The simulations with the use of the detailed kinetic mechanism predicts

76 higher combustion efficiency than the calculations using the one-step model.
77 The comparison of wall static pressure from the experiments and the numer-
78 ical simulations showed that the detailed and the single step chemistry give
79 similar results and predict well the positions of pressure peaks, but they fail
80 to predict the values of pressure peaks. All the numerical simulations were
81 carried out using software package Fluent [2].

82 The use of a detailed mechanism should give a more precise estimation of
83 the main thermodynamic parameters: temperature and pressure, and should
84 provide the distribution of the intermediates: OH, H₂O₂, etc. Generally
85 detailed kinetic model provides much more information about combustion
86 processes, but the use of it costs an additional CPU power.

In the considered above work Kumaran and Babu used the kinetic mech-
anism of Stahl and Warnatz [9] published in 1985 as the reference detailed
mechanism. This mechanism became a little bit old after publication of
works [10, 11] in 2002. In these works the refined data on the rate constant
of reaction R9 [10]



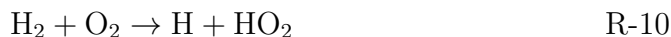
and the enthalpy of formation of OH [11] were reported. Since radicals OH
and HO₂ play the essential role in hydrogen oxidation, all kinetic mechanisms
developed before 2002 should be revised. In the current work the several de-
tailed hydrogen kinetic mechanisms are tested. One is “old” [12], while three
others [13, 15, 16] were released after 2002. Besides the outdated thermo-
dynamic data and the outdated rate constants “old” mechanism [12] has
reaction:



87 The usage of this reaction became marginal nowadays, for example: it is
88 not included into modern mechanisms [13]-[15] considered below. The “old”
89 mechanism has been tested in order to see the difference from the updated
90 mechanisms.

91 Konnov reported recently about “remaining uncertainties in the kinetic
92 mechanism of hydrogen combustion” in work [13]. He studied the detailed
93 hydrogen combustion mechanism. Konnov found two groups of the uncer-
94 tainties. The first group is associated with the set of the chemical reactions
95 in the hydrogen–oxygen system. Not all of the possible reactions are in-
96 cluded in the kinetic mechanisms, and the set of reactions varies from one
97 mechanism to another. Thereby there is no one conventional set of reactions,
98 which describes combustion of hydrogen comprehensively, and this problem
99 is still open. The second type of uncertainties relate to the uncertainties in
100 the rate constants of the employed reactions. Some of them are not well
101 defined or the experimental data on them are controversial. It should be
102 noted that developed by Konnov hydrogen kinetic mechanism [14] has the
103 slightly different set of reactions from others extensively cited mechanisms
104 from Princeton University [17], National University of Ireland, Galway [15],
105 etc.

Shatalov et al. [18] carried out the analysis of several detailed kinetic
mechanisms of hydrogen combustion: the mechanism by Konnov [13] and
mechanisms by other authors. Shatalov et al. [18] noted that the use of
reaction RX does not have a sense, because another parallel channel



106 has the significantly greater rate constant (in 50 and more times). On the

107 other hand the use of reaction RX helps a lot to fit experimental data. They
108 pointed out also that below 1100 K reaction R9 effects on the ignition delay
109 time significantly.

110 There are two very recent hydrogen reaction mechanisms from Princeton
111 and Stanford universities [16, 19]. The both are validated against the latest
112 experimental data. For our applications (rocket combustion) the experi-
113 mental data of Burke and coworkers [20] (the same team as [16]) is the
114 most interesting. This experimental data represents the measurements of
115 the burning velocities in $H_2/O_2/He$ mixtures at pressures 1–25 atm. These
116 measurements are the only available data for hydrogen at high pressure. The
117 comparisons of these recent mechanisms with the experimental data showed
118 that the mechanism by Burke *et al.* [16] has a better agreement with ex-
119 perimental data at high pressure than mechanism [19]. By this reason only
120 mechanism by Burke *et al.* [16] has been chosen for the tests in this work.

121 A study similar to the current work was carried out by Gerlinger *et al.*
122 [21]. The colleagues studied several hydrogen/air reaction mechanisms in-
123 cluding multi-step schemes [7, 15, 22] and one-step mechanism by Marinov
124 *et al.* [23]. The study is focused in the application of reaction mechanisms
125 in the simulation of supersonic combustion. The mechanisms were validated
126 against ignition delay times. In the validation all mechanism showed sim-
127 ilar results excluding one-step mechanism [23], which missed a non-Arrhenius
128 behavior of the experimental data. The authors simulated supersonic com-
129 bustion with the different mechanism and compared the results with an ex-
130 perimental data. They studied the influence of timestep and numerical grid
131 as well. The numerical results showed the sensitivity to the timestep and the

132 grid density. Finally the authors conclude that one-step mechanism [23] is
133 not appropriate, while mechanism by O’Conaire *et al.* [15] is more precise
134 than other multi-step mechanisms.

135 While the examples of successful verification, validation and application
136 of hydrogen reaction mechanisms in CFD simulation of supersonic combus-
137 tion ramjet exist, the problem of the CFD simulation of hydrogen combustion
138 in rocket engine is not closed. Scramjet is a specific case and the results ob-
139 tained for supersonic combustion cannot be extended over the case of rocket
140 engine. Combustion in rocket engine has its own characteristic features:
141 high pressures (50–250 atm), the wide span of temperatures from 100 K
142 to 3500 K, the absence of dilutant (nitrogen). In the case of scramjet the
143 verification and validation can be done by simulating a supersonic combus-
144 tion directly what is not possible in the case of combustion in rocket engine
145 yet. In recent work [24] the group of researchers from five research cen-
146 ters made the CFD simulations of a flow in a combustion chamber. The
147 each participant of the project modeled the same object using own meth-
148 odology. It was the sub-scale rocket engine with 1.5 inch inner diameter,
149 with one co-axial injector. The combustion chamber had an axial symmetry,
150 which allowed to carry out the comparison of 2D and 3D modeling. The au-
151 thors compared steady Reynolds–Average Navier–Stockes (RANS), unsteady
152 Reynolds–Average Navier–Stockes (URANS) and three different Large Eddy
153 Simulation (LES) models with the experiment. The comparison showed that
154 all approaches give the noticeably different results and the only in one case
155 (LES — stochastic reconstruction model) the obtained results were compar-
156 able with the experimental data. Indeed the most precise modeling results

157 were obtained with the finest mesh of $255 \cdot 10^6$ cells and using the highest
158 computational power of 2 million cumulative CPU hours. However at the
159 current moment it is not totally clear how the initial model assumptions af-
160 fected the accuracy of the final results, and what assumption or parameter
161 impaired the other models. Such comparison is very important from the
162 practical point of view because the computational cost and precision vary
163 strongly from one numerical model to another.

164 The performance of the chemical kinetic models of hydrogen oxidation
165 in CFD simulations has been estimated in the current work. The aims of
166 the work are the ranking of the selected hydrogen kinetic models and the
167 development of the verification, validation and ranking procedures. In the
168 current work the performance of the kinetic models are assessed using the
169 experimental data on hydrogen ignition [25] and hydrogen flame [26]. The
170 CFD simulations are carried out using complex physical models. In such con-
171 ditions the all-round verification is simply obligatory for the CFD modeling,
172 while there is no conventional way to verify combustion models as a part of
173 the whole physical-chemical model as well as no conventional way to verify
174 and validate physical model itself so far. The simulations have a secondary
175 aim to estimate the validity region within the space of the computational
176 parameters: mesh, computational scheme, time step. The precision (the dif-
177 ference between calculations and experiments) and the computational cost
178 (required CPU time) were estimated on the each test case. Global reaction
179 model [23], two-step scheme [31], abridged Jachimowski's model [22], a new
180 skeletal mechanism, four detailed hydrogen mechanisms [12, 13, 15, 16] have
181 been tested. Thus the results of the work should show what chemical kinetic

182 scheme should be used, at which parameters the scheme should be used, how
183 much computing power it is necessary to have for the fulfilment of a task.
184 The work is the first step before the CFD simulations of the experiments
185 carried out at our test facility [29, 30].

186 **2. Skeletal kinetic model**

187 In our case as well as in other CFD simulations the numerical and the
188 physical models have a lot of parameters and need the debugging before
189 getting the final solution. Parameters, which are not connected with the
190 problem directly, for example timestep, can seriously obstruct the obtaining
191 of a solution. Detailed kinetic mechanisms make CFD models too heavy for
192 the debugging. On the other side global reaction models do not include the
193 minor species and do not allow to do the all-round debugging (validation and
194 verification of the properties of HO_2 , H_2O_2 , etc.).

195 In this work a skeletal kinetic scheme has been developed, which has the
196 same set of species as detailed hydrogen mechanisms, but the reduced set
197 of reactions. This light scheme sped up the formulation of the computa-
198 tional problem. The problem definition requires to perform the certain set of
199 the calculations. Different meshes and the models of diffusion and thermal
200 conductivity were tried before getting the final results. The light skeletal
201 scheme reduced the amount of the expended CPU hours at the preliminary
202 stage. The new scheme fills the gap between abridged Jachimowski's model
203 [22], which has 7 reactions and 6 species, and detailed hydrogen mechanisms
204 [12, 14, 15] (19–21 reactions, 8 species and bath gases) as well as it allows to
205 separate the influence of the amount of reactions and species.

The new scheme was developed from the skeletal model by Kreutz and Law [32]. Their skeletal kinetic model has 9 unidirectional reactions and 8 species. Considering H_2/O_2 system it may assume that the set of 9 species: H_2 , O_2 , H_2O , H , O , OH , HO_2 , H_2O_2 and bath gas is complete and other species (O_3 , OH^- , $\text{OH}^*(\text{A})$, etc.) can play role only in marginal cases. It is necessary to note that at high pressures, what is the case of rocket combustion chambers, the chain branching proceeds via the formation of HO_2 , H_2O_2 radicals due to the high rates of the recombination processes [33]. For example reaction



which is the most important in atmospheric hydrogen flames, is suppressed by reaction R9 at pressures above 50 bar. The model by Kreutz and Law [32] has a 5 times smaller set of reactions as detailed hydrogen mechanisms and can adequately predict the ignition delay times and the ignition limits. On the other hand the scheme consists of the irreversible reactions, which means that the concentrations of species never reach the equilibrium state. The afterburning processes are omitted, which is not important during ignition, but leads the mispredictions of species profiles. By these reason the reaction set was extended by 6 reactions from detailed hydrogen model [15]. The reaction of the quadratic recombination of HO_2 radicals



206 was substituted by reactions R11 and R13, see Tables 1, 2. Such extension
 207 increases the computational weight of the model, but it increases the ad-
 208 equacy of the model as well. The new added reactions involve the processes
 209 of radical recombinations, which are important in a post flame zone.

210 3. Calculations

211 The CFD calculations have been done with the use of the ANSYS CFX
212 11 solver [1], which utilizes the Finite Volume Element Method (FVEM).
213 The meshes have been created using ANSYS ICEM software. The choice of
214 the software is given by an adherence to the compatibility of the computer
215 data and the design documentation.

216 Two types of tests (simulations) have been done in the work. The first
217 test case is a quasi 0-dimensional simulation of hydrogen ignition to verify
218 and validate the models against the experimental data on ignition delay times
219 [25]. The second test case is an 1-dimensional simulation of hydrogen flame
220 propagation to test the models against the data on the speeds of laminar
221 flame [26].

222 An ignition in a perfect adiabatic constant volume reactor has been
223 modeled as the quasi 0D problem. By the formulation the problem is di-
224 mensionless, but by the settings of calculations it is 3D. The computational
225 domain represents eighth part of the 1 mm sphere with rigid adiabatic walls.
226 The mesh consists of 21 nodes and 38 tetrahedron elements. At the ini-
227 tial moment the whole domain is filled with a stoichiometric hydrogen–air
228 ($0.79\text{N}_2+0.21\text{O}_2$) mixture at pressure of 1 atm and temperature in the range
229 of 900–1400 K. The problem has been solved as a transient task, i.e. the time
230 evolution of gas conditions has been sought. The laminar model (unsteady
231 Navier–Stokes equations) was employed, but also one series of simulations
232 were carried out using the k - ϵ turbulence model. The comparison of results
233 shows that both models (the laminar and the k - ϵ model) give the same results
234 in this task. The task was imposed in such way that the results should be

235 independent on the choice of turbulence model. Indeed the stagnant homo-
236 geneous gas mixture is surrounded with the adiabatic rigid walls, so the gas
237 inside the sphere should be stagnant all time. The object of these calcula-
238 tions is the estimation of the ignition delay times and the comparison of the
239 calculated delay times with the data from shock tube experiments [25], see
240 Fig. 2. In the calculations the ignition delay times were defined as the time
241 of a temperature increase up to 500 K relative to the initial temperature.

242 During the 1D tests a freely propagating hydrogen flame has been modeled.
243 The computational domain consists of 1604 nodes and 400 rectangular prism
244 elements. All elements are placed along one axis so that the thickness of
245 the domain equals to one element in two other coordinate axes. The mesh
246 spacing equals to 5 μm in the direction of the flame propagation. The sep-
247 arate study of the influence of the grid spacing was carried out where the
248 spacing was varied from 0.2 μm to 200 μm . The domain represents the rect-
249 angular with symmetry boundary conditions on the side walls. The domain
250 has one inlet and one outlet (on the side opposite to inlet). At the outlet
251 static pressure is specified and equals to 1 atm. At the inlet a hydrogen–air
252 (0.79N₂+0.21O₂) mixture at 298 K and 1 atm flows inside the domain. The
253 velocity of the mixture is specified at the inlet in the range of 0.5–3.5 m/s so
254 that the velocity of the flame front reaches a small value in the laboratory
255 system of coordinates. The mixture composition was varied from equival-
256 ence ratio of ER = 0.5 to ER = 4.5. The simulations were run as a transient
257 task. A stationary burning velocity was sought. The laminar model was
258 employed, also one series of tests were carried out using the k - ϵ turbulence
259 model. Speed of flame depends essentially on the transport properties of gas,

260 so the temperature dependent thermal conductivity and diffusion coefficients
261 were used. Thermal diffusion was not taken into account. The system of the
262 governing equations in ANSYS CFX does not assume mass fluxes caused by
263 temperature gradients.

264 4. Results and discussion

265 4.1. Verification. Comparison with CHEMKIN.

The both tasks were also solved in CHEMKIN II [5]. The results of the simulations with the help of CHEMKIN II were used as a reference data. CHEMKIN is very widely used for solving chemical kinetic problems, where the computational problem is formulated as solving of a system of ordinary differential equations. Indeed ANSYS CFX allows to specify the properties of a system by the different ways, while in CHEMKIN task is set in the one prescribed format. CHEMKIN uses the modified Arrhenius form for rate coefficients:

$$k = A \cdot T^n \cdot \exp(-E_a/RT).$$

266 The thermodynamic functions: enthalpy, entropy and heat capacity are cal-
267 culated using the NASA polynomial forms in CHEMKIN. During the cal-
268 culations in ANSYS CFX the same equations were employed for the rate
269 constants, the thermodynamic functions and the equations of states, so the
270 comparisons of the results obtained using the different software have a sense.
271 The results of the comparisons is depicted in Fig. 3 and Fig. 4, where ANSYS
272 CFX shows the agreement with CHEMKIN.

273 Using CHEMKIN the ignition delay times were calculated in the assump-
274 tions of constant volume and adiabatic walls. In this case the problem defin-

275 itions (the sets of boundary conditions and kinetic equations) correspond
276 to each other in ANSYS CFX and CHEMKIN. As a consequence the res-
277 ults of the simulations using ANSYS CFX agree fully with the computa-
278 tions in CHEMKIN, see Fig. 3. Indeed it is necessary to note that CFX
279 solves the 3-dimensional Navier–Stokes equations while CHEMKIN uses the
280 0-dimensional equation of energy conservation.

281 The next step is the modeling of freely propagating laminar flame. Zeldovich–
282 Frank-Kamenetskii equation, which connects flame velocity and reactivity,
283 gives us a clear view on the problem:

$$u_{lam} = \sqrt{\frac{\alpha}{\tau}}, \quad (1)$$

284 where τ is the chemical time scale in reaction zone, and α is the coefficient
285 of temperature conductivity, which summarizes the effect of diffusion and
286 heat conductivity through Lewis number $Le = 1$. In contrast to the previ-
287 ous case kinetic and transport properties have an equal importance in flame
288 propagation.

289 The flame speeds were estimated using ANSYS CFX and PREMIX [27],
290 Fig. 4. PREMIX is a subroutine of the CHEMKIN which computes species
291 and temperature profiles in steady-state laminar flames. The transport prop-
292 erties were estimated using TRANFIT: the another part of the CHEMKIN
293 collection. Thermal conductivity, viscosity and diffusion coefficients are es-
294 timated from the parameters of the Lennard–Jones potential and the dipole
295 moment of species. The same temperature depended coefficients of thermal
296 conductivity, viscosity and binary diffusion were used in PREMIX and AN-
297 SYS CFX, but diffusion fluxes in multicomponent mixture were approxim-
298 ated by a different way.

299 The specific of H₂-O₂ system is that the properties of hydrogen (the
 300 lightest gas) distinguishes strongly from the properties of other species within
 301 the system. By default ANSYS CFX estimates the transport properties in
 302 the mixture of gases by an inappropriate way for H₂-O₂ system, where the
 303 influence of the fuel on the transport properties is important. It calculates the
 304 coefficient of thermal conductivity and viscosity of gas mixture using a mass
 305 averaging, and the coefficients of diffusion are calculated from the mixture
 306 bulk viscosity. The problem becomes significant in the case of combustion
 307 in rocket engine where the mixture is not diluted by nitrogen. This problem
 308 can be resolved in ANSYS CFX using CFX Expression Language (CEL) and
 309 setting all coefficients by user as it was done in this work.

310 In H₂-O₂ system the diffusion coefficients vary from one component to
 311 other in ~ 6 times: $D_{O_2}/D_H \approx \sqrt{(\mu_{O_2}/\mu_H)} \approx \sqrt{32}$. Even in the simplest
 312 case, where only H₂, O₂, H₂O are taken into account, the gas mixture can
 313 not be assume as a binary mixture or as a solution of light gas in heavy gas
 314 due to the high fractions of H₂ and H₂O and the differences in the diffusion
 315 coefficients. In the current work the diffusion coefficients are calculated by
 316 the empirical formula

$$D_i = \frac{1 - w_j}{\sum X_j / D_{ij}}, \quad (2)$$

317 where w_i is the mass fraction of i-species; X_j is the mole fraction of j-species;
 318 D_{ij} is the binary diffusion coefficient [34]. After that the diffusion coefficients
 319 of individual species are put into the equation which is responsible for the
 320 transport in CFX:

$$\rho_i(U_{mix} - U_i) = -\frac{D_i}{\rho_{mix}} \frac{\partial \rho}{\partial x}, \quad (3)$$

321 where $\rho_i(U_{mix} - U_i)$ is the relative mass flux of i-species. The equation is

322 not solved for an one constraint component (in our case nitrogen), which
323 mass fraction is calculated from the constraint that the sum of mass frac-
324 tions of all species equals to 1. PREMIX (CHEMKIN) uses a more accu-
325 rate definitions of the diffusion and the thermal conductivity in gas mixture,
326 and takes into account the thermal diffusion of H and H₂. There are two
327 options: “mixture-averaged properties” and “multicomponent properties”
328 in PREMIX. “Mixture-averaged” option, which was used here, employ eq.
329 (2), but does not have a constraint species and employs an additional term
330 — correction velocity, which makes the net species diffusion flux equal to
331 zero. “Multicomponent” formulation uses the method described by Dixon-
332 Lewis [28], where the coefficients are computed from the solution of a system
333 of equations defined by the L matrix.

334 The flame velocities obtained with the use of CFX and CHEMKIN coin-
335 cide practically with each other. The difference in the results, which is small
336 (Fig. 4), should be associated with the distinction between the formulations
337 of the diffusion fluxes. Coffee and Heimerl [35] compared various methods of
338 approximating the transport properties of premixed laminar flames, in par-
339 ticular the methods which have been used in CFX and CHEMKIN. They
340 found that the difference in flame speed is small for these methods, but
341 the method, which is employed in CHEMKIN, is more accurate than the
342 method with constrained species (CFX), which is inaccurate in computing
343 the diffusion velocity for constrained species. As for the comparison with
344 experimental data it was shown in recent work [36] that such small over-
345 shooting around the stoichiometry, which is observed in Fig. 4, results from
346 the neglecting Soret effect (thermodiffusion).

347 In our case (laminar hydrogen–air flame at 1 atm) the propagation of the
348 flame is supported essentially by the diffusion H_2 into flame zone and the
349 diffusion of H into preflame zone. That is why it is important to estimate
350 accurately the diffusion term. in Fig. 5 we can see the effect of the transport
351 properties on laminar flame. The maximum of the flame speed is shifted to
352 the higher equivalent ratios where the diffusive fluxes of H and H_2 are higher.

353 4.2. Validation and testing

354 Let us consider the results of the first “0D” test case, which is depicted in
355 Fig. 2. The detailed models [12, 14–16] agree with experimental data well,
356 while non-detailed kinetic models [23, 31], abridged Jachimowski’s model
357 [22] and the new skeletal model have the agreement with experimental data
358 only in the limited range. The kinetic model by Konnov [13] agrees with
359 experimental data better than other models. In Fig. 2 it is possible to see
360 the transition from high–temperature kinetics to low–temperature kinetics
361 around 950 K. Generally the models show the common trend: more details
362 — higher accuracy. This conclusion is supported by the results of the 1D
363 test case too. It is possible to conclude from the results that one or two
364 reactions are not enough to describe the ignition of hydrogen. Probably the
365 sophistication of abridged Jachimowski’s model (7 reactions and H, O, OH as
366 intermediates) is a reasonable minimum for the modeling of hydrogen com-
367 bustion in the high temperature region ($T > 1000$ K). For the modeling in a
368 wide temperature range the formation of H_2O_2 and HO_2 should be taken into
369 account. Of course it would be very surprising to see that reduced or global
370 mechanisms can describe ignition in a wide range of parameters. They are
371 deduced from detailed mechanisms by neglecting the marginal processes, so

372 they can not describe the behavior near margins. In most cases the oxidation
373 of hydrogen proceeds via the formation of HO₂ radical, which is not included
374 in the reduced mechanisms. In the new mechanism the kinetics of HO₂ is
375 not comprehensive too.

376 It is necessary to note that shock tube is not a reactor with adiabatic
377 solid walls. Due to the boundary layer effect the temperature behind re-
378 flected shock wave slowly increases with time. The discrepancy between the
379 ideal assumptions and reality arise at large residence times, for the most of
380 the shock tubes after 1 ms. In Fig. 2, where the ignition delay times are cal-
381 culated using the boundary conditions of adiabatic solid walls, the detailed
382 models have a “wrong” trend at low temperatures (large residence times).
383 At large residence time it is necessary to take into account the real conditions
384 behind reflected shock wave as it was done in [19]. In this case the actual
385 agreement between experiments and detailed models [14–16] will better than
386 on the graph.

387 The performed simulations give more information about the evolution of
388 the system than simply ignition delay times. The “classical” behavior was
389 observed without anything unusual in the all “0D” tests (by this reason it is
390 not included in the article). All the kinetic models predict similar temper-
391 ature (or pressure) time-resolved profiles, which have the induction period,
392 the following temperature (or pressure) rise, which ends with asymptotic be-
393 havior. The gas temperature (or pressure) of the combustion products is
394 predicted correctly by the all kinetic models.

395 In the 1D test case the agreement of the simulating data with the ex-
396 perimental data is better in sum than in the “ignition” case, see Fig. 5.

397 Practically the all models agree with the experimental data. The other dis-
398 tinctive feature of the obtained results is the bad agreement of abridged
399 Jachimowski's model [22] and the good agreement of one-step model [23].
400 The results of 1D simulations can be interpret in terms of eq. (1). The sys-
401 tem has practically the same physical properties in the all 1D simulations.
402 These allow us to conclude that

$$\frac{u_1}{u_2} = \sqrt{\frac{\tau_2}{\tau_1}}, \quad (4)$$

403 where indexes *1* and *2* designate the attribute to different kinetic models.
404 The ignition delay times should be taken at flame temperature. In our case
405 the flame temperature amounts ~ 2000 K. Abridged Jachimowski's model
406 [22] has the lowest effective activation energy among the models (see Fig. 2)
407 and predicts the significantly larger τ at high temperatures. As for one-step
408 model [23], which predicts the shortest τ at high temperatures, it does not
409 include atomic hydrogen. It means that the assumptions, which lead us to
410 eq. (4), are not correct for this model. In terms of eq. (1) the neglecting of
411 the diffusion of hydrogen atom should lead to the smaller value of α and to
412 the essentially less flame velocity, but it is compensated in this model by the
413 small ignition delay time.

414 In Figures 2 andb 5 we can see the difference between the results of the
415 simulations and the experiments. While in the case of the global or reduced
416 kinetic models the discrepancy can be attributed to the weakness of models,
417 detailed reaction mechanisms [12, 14, 15] represent the state-of-the-art view
418 on hydrogen kinetics. The agreement of these models with experimental data
419 and the role of intermediates (H, O, OH, HO₂ and H₂O₂) were discussed in
420 details in original articles [12, 14, 15]. The oxidation of hydrogen proceeds

421 via the formation of highly active intermediates. The experimental study
422 of the kinetics of the intermediates of H_2/O_2 system has some difficulties
423 at temperatures below 900 K where in experiments it is necessary to keep
424 constant conditions during long residence times. Thus even a detailed kinetic
425 scheme can fail near ignition and flammability limits.

426 Numerical parameters such as time step, grid spacing, type of difference
427 scheme, etc. should not determine the results of modeling. The proper values
428 of time step and grid spacing should correspond via the coefficients of physical
429 model to physical time and space scales. On practical ground the upper limits
430 of time step and grid spacing are more important, because computational cost
431 is generally inversely proportional to timestep and the amount of nodes (for
432 the employed grid the amount of nodes is reciprocally proportional to the
433 grid spacing), see Fig. 6. The employed values of time step and grid spacing
434 are normally close to the upper limit. Generally chemical processes can not
435 be faster than several fractions of microsecond, and hydrodynamic processes
436 can not take place on a scale smaller than a micrometer. Thus these values
437 can be set as a reasonable lower limit for the time step and the grid spacing.
438 The upper limit is quite specific to the details of a task. It is necessary to
439 estimate the maximum time and mesh steps in each case separately. At a
440 too high time step the solution diverges. Numerical noise and residuals can
441 be used as the measure of the proximity to the upper limit of time step. In
442 this work the adaptive time step has been used and it has been defined by
443 a residual. The time step was decreased or increased until the value of the
444 residuals reached the desired level. To estimate the upper limit of mesh step
445 several simulations were carried out with different spacing, see Fig. 6. On

446 the plot we can see a plateau for the cell size below 5 μm . The upper limit,
447 which is located near 10 μm , is related to the flame thickness. In flame front
448 the concentration of hydrogen increases in 2–4 times each 10 μm . Probably
449 the maximum grid spacing is universal for all hydrogen–air flames at 1 atm
450 and is defined by the transport properties of the system while the maximum
451 time step is individual for each kinetic model. As we can see later, maximum
452 time step is related to the stiffness of kinetic scheme.

453 Grid spacing, the physical dimensions of computational domain and com-
454 putational cost are connected with each other. At these conditions grid spa-
455 cing can limit the applicability of kinetic model. In Table 3 the computational
456 costs, which are required for the simulation of the evolution of the system
457 during 1 ms on 1 CPU (Pentium 4) at 2 GHz, are presented for the all tested
458 models. In the identical the conditions computational cost varies by orders
459 from one model to another. It is impossible from the data of Table 3 to see
460 any direct connection of the computational cost with the number of reac-
461 tions and species. However there is a trend: detailed kinetic models require
462 a much more computational power than reduced models. Thus the high com-
463 putational cost limits the application of detailed kinetic mechanisms in CFD
464 calculations seriously. The grid spacing has the limit near 40 μm after which
465 the simulations give the absolutely unrealistic results. Detailed models can
466 be employed only in a special tasks with the computational domains of small
467 sizes due to the high computational cost and the small grid spacing.

The computational cost increases strongly from the global reaction mod-
els to the detailed kinetic mechanisms, but the number of chemical equations
and species does not completely determine computation cost. Another es-

sential parameter is the stiffness of kinetic model. Stiffness is the embedded parameter of each kinetic model. It determines the maximum timestep during calculations. It arises due to differences in timescales for different chemical reactions. To solve kinetic equations it necessary to integrate equations using timestep related the smallest timescale over the time interval related to the largest timescale. Stiffness can be characterized the ratio of timescales. For example, reaction R9 is in 10^{10} times faster than reaction



in preflame zone while in postflame zone it is vice versa, reaction R1 is faster than reaction R9 in 100 times. It is typical for combustion problems, when important fast reactions run on the background of slow equally important processes. Another example of the embedded stiffness is reaction



468 This reaction determines concentration of H_2O_2 in flame, and it changes its
469 direction from reverse to forward after passing the flame front.

470 5. Conclusions

471 The eight different kinetic models of hydrogen oxidation were verified,
472 validated and tested in the CFD simulations what was done using ANSYS
473 CFX 11 software. The two cases: ignition in adiabatic constant volume
474 reactor and the propagation of free laminar flame were considered. The
475 verification of the kinetic models was done through the comparison with the
476 results obtained with the help of the Chemkin software. The verification

477 allowed to eliminate misentries and to define correctly the thermodynamic,
478 kinetic and transport properties.

479 The subsequent validation showed that the detailed kinetic schemes are
480 more precise than the reduced. While it was not found any dependence
481 between the "speed" of kinetic model and the number of reaction and species,
482 the reduced kinetic scheme are faster than detailed. The simulations showed
483 the common trend for kinetic models: more details — higher computational
484 cost — higher precision. The simulation of the ignition of hydrogen–air
485 mixture showed that the results are sensitive to the choice of kinetic model.
486 However in the case of the flame propagation the results are more sensitive
487 to the model of the transport properties while the reasonable results can be
488 achieved even with the use of global reaction mechanism.

489 The comparison of the simulating data with the experimental data [25, 26]
490 showed that detailed kinetic schemes [14–16] agree with experiments well,
491 while the non-detailed schemes agree with the experiments only within a
492 limited range. The kinetic model by Konnov [14] has the best agreement
493 with the experimental data among the tested models. The application of
494 reduced kinetic schemes of hydrogen combustion, which do not take into
495 account chemical reactions with HO_2 and H_2O_2 , is possible only with strong
496 limitations.

497 For the debugging purposes the new skeletal kinetic scheme was developed
498 which represents the good compromise between computational cost and ac-
499 curacy.

500 The carried out study showed that computational results are affected
501 by the parameters of physical and numerical models. A large amount of

502 model parameters is the potential source of errors. The number of different
503 coefficients reaches thousands in the simulation with the use of a detailed
504 kinetic model. The parameters of the model can be verified and validated
505 using the proposed method.

506 The application of kinetic models in CFD calculations requires the con-
507 siderable amount of computational power. The maximum time is limited by
508 the stiffness of model and alters from model to model while the maximum
509 grid spacing is more or less universal and defined by the thickness of flame
510 front.

511 **Acknowledgments**

512 The author is grateful to Andreas Gernoth for introducing into ANSYS
513 CFX. Also the author appreciate the scientific discussions with Dr. Oskar
514 Haidn.

515 **References**

- 516 [1] ANSYS CFX, <http://www.ansys.com/products/cfx.asp>
- 517 [2] Fluent, <http://www.fluent.com/>
- 518 [3] Star-CD, <http://www.cd-adapco.com/products/STAR-CD/>
- 519 [4] Roache, P.J., "Verification of Codes and Calculations," AIAA Journal,
520 Vol. 36, No. 5, May 1998, pp. 696-702.
- 521 [5] Kee, R. J., Rupley, F. M., and Miller, J. A., "CHEMKIN-II: A Fortran
522 Chemical Kinetics Package for the Analysis of Gas-Phase Chemical Kin-
523 etics", Sandia National Laboratories Report, SAND89-8009, 1989.
- 524 [6] Mani, M., Bush, R.H., Vogel, P.G., "Implicit Equilibrium and Finite-
525 Rate Chemistry Models For High Speed Flow Applications," AIAA Pa-
526 per 91-3299-CP, Jan. 1991.
- 527 [7] C.J. Jachimowski, An analytical study of hydrogen-air reaction mech-
528 anism with application to scramjet, NASA Technical Paper 2791 (1988)
529 Feb.
- 530 [8] K. Kumaran, V. Babu, Combust.Flame 156 (2009) 826-841.
- 531 [9] G. Stahl, J. Warnatz, Combust.Flame 85 (3-4) (1991) 285-299.
- 532 [10] Michael, J. V.; Su, M. C.; Sutherland, J. W.; Carroll, J. J.; Wagner, A.
533 F. J Phys Chem A 2002, 106, 5297.

- 534 [11] Ruscic, B.; Wagner, A. F.; Harding, L. B.; Asher, R. L.; Feller, D.;
535 Dixon, D. A.; Peterson, K. A.; Song, Y.; Qian, X.; Ng, C.; Liu, J. Chen,
536 W.; Schwenke, D. W. *J Phys Chem A* 2002, 106, 2727.
- 537 [12] Gutheil, E., Balakrishnan, M.D., Williams, F.A., "Structure and Ex-
538 tinction of Hydrogen-Air Diffusion Flames", *Reduced Mechanisms for*
539 *Application in Combustion Systems*, Springer-Verlag, Berlin, Heidel-
540 berg, 1993.
- 541 [13] A.A. Konnov, *Combust. Flame* 152 (4) (2008), pp. 507-528.
- 542 [14] Konnov, A.A., Development and validation of a detailed reaction mech-
543 anism for the combustion of small hydrocarbons. 28-th Symposium (Int.)
544 on Combustion, Edinburgh, 2000. *Abstr. Symp. Pap.* p. 317.
- 545 [15] M. O'Conaire, H.J. Curran, J.M. Simmie, W.J. Pitz and C.K. West-
546 brook, *Int. J. Chem. Kinet.* 36 (2004), pp. 603-622.
- 547 [16] M.P. Burke, M. Chaos, Y. Ju, F.L. Dryer, S.J. Klippenstein, *Int. J.*
548 *Chem. Kinet.* (2011).
- 549 [17] J. Li, Z. Zhao, A. Kazakov and F.L. Dryer, *Int. J. Chem. Kinet.* 36
550 (2004), pp. 566-57.
- 551 [18] O.P. Shatalov, L.B. Ibraguimova, V.A. Pavlov et al., Analysis of the
552 kinetic data described oxygen-hydrogen mixtures combustion, *Proceed-*
553 *ings of the 4th European Combustion Meeting*, Vienna, Austria, 14-17
554 April, 2009.

- 555 [19] Hong, Z.; Davidson, D. F.; Hanson, R. K. *Combust Flame* 2011, 158,
556 633-644.
- 557 [20] Burke, M. P.; Chaos, M.; Dryer, F. L.; Ju, Y. *Combust Flame* 2010,
558 157, 618631.
- 559 [21] Gerlinger, P., Nold, K., and Aigner, M., *Int. J. Numer. Meth. Fluids*
560 2010; 62:13571380.
- 561 [22] Eklund D.R. ,Stouffer S.D., A numerical and experimental study of a
562 supersonic combustor employing swept ramp fuel injectors. *AIAA Paper*
563 94-2819, 1994.
- 564 [23] Marinov, N.M., Westbrook, C.K. and Pitz, W.J., *Detailed and Global*
565 *Chemical Kinetic Model for Hydrogen, Transport Phenomena in Com-*
566 *Combustion Volume 1*, Taylor and Francis, Washington DC, 1996.
- 567 [24] P.K. Tucker, S. Menon, C.L. Merkle, J.C. Oefelein, V. Yang, 44-th
568 *AIAA/ASME/SAE/ASEE Joint Propulsion Conference & Exhibit*, 21-
569 23 July 2008, Hartford, CT USA, *AIAA* 2008-5226.
- 570 [25] Slack, M., Grillo, A., *Investigation of Hydrogen-Air Ignition Sensitized*
571 *by Nitric Oxide and by Nitrogen Oxide*, *NASA Report CR-2896*, 1977.
- 572 [26] Kwon, O.C., Faeth, G.M., *Combust. Flame*, 124 (2001) 590-610.
- 573 [27] Kee, R.J., Grcar, J.F., Smooke, M.D., and Miller, J.A., "A Fortran
574 Program For Modeling Steady Laminar One-Dimensional Premixed
575 Flames", *Sandia National Laboratories Report*, SAND89-8240, 1985.

- 576 [28] Dixon-Lewis, Proc. R. Soc. Lond. A October 15, 1968 307:111-135.
- 577 [29] Gurliat, O., Schmidt, V., Haidn, O.J., Oschwald, M., Aerospace Science
578 and Technology 7 (2003) 517–531.
- 579 [30] Suslov, D., Lux, J., Haidn, O., Investigation of porous injector elements
580 for LOX/CH₄ and LOX/H₂ combustion at sub- and super-critical con-
581 ditions, 2nd European Conference for Aerospace Sciences 1–6 July, 2007,
582 Brussels, Belgium.
- 583 [31] Lee, S.R., Kim, J.S., Korean J. Chem. Eng. 16(2) (1999) 253–259.
- 584 [32] Kreutz T.G. and Law C.K., Combust. Flame, 114:436–456, 1998.
- 585 [33] Zhukov, Victor P.(2009)'Kinetic model of alkane oxidation at high
586 pressure from methane to n-heptane',Combustion Theory and Model-
587 ling,13:3,427442. DOI: 10.1080/13647830902767302
- 588 [34] J. Warnatz, U. Maas, R.W. Dibble, Combustion, Springer–Verlag, Ber-
589 lin, Heidelberg, New York, 1996.
- 590 [35] Coffee, T.P., and Heimerl, J.M., Combust.Flame 43 (1981) 273–289.
- 591 [36] F. Yang, C.K. Law, C.J. Sung, H.Q. Zhang, Combust.Flame 157 (2010)
592 192–200.

Table 1: New skeletal mechanism.

No	Ref. No	Reaction	A	n	E _a	Ref.
1	R1	H + O ₂ → OH + O	1.91e+14	0.0	16.44	[32]
2	R2	H ₂ + O → H + OH	5.08e+4	2.67	6.292	[32]
3	R3	H ₂ + OH → H + H ₂ O	2.16e+8	1.51	3.43	[32]
4	R5	H ₂ + M ↔ H + H + M	4.57e+19	-1.4	105.1	[15]
5	R6	O + O + M ↔ O ₂ + M	6.17e+15	-0.5	0.0	[15]
6	R7	H + O + M → OH + M	4.72e+18	-1.0	0.0	[15]
7	R8	H + OH + M → H ₂ O + M	4.5e+22	-2.0	0.0	[15]
8	R9	H + O ₂ + M → HO ₂ + M	6.17e+9	-1.42	0.0	[32]
9	R10	H + HO ₂ → H ₂ + O ₂	1.66e+13	0.0	0.82	[15]
10	R-10	H ₂ + O ₂ → H + HO ₂	3.68e+13	0.203	54.46	[32]
11	R11	H + HO ₂ → OH + OH	1.69e+14	0.0	0.87	[32]
12	R13	OH + HO ₂ → H ₂ O + O ₂	2.89e+13	0.0	-0.5	[15]
13	R15	H ₂ O ₂ + M → OH + OH + M	1.2e+17	0.0	45.5	[32]
14	R-17	H ₂ + HO ₂ → H + H ₂ O ₂	3.42e+12	0.202	27.12	[32]

$k = A \cdot T^n \cdot \exp(-E_a/RT)$; units: mol, cm³, K, kcal; thermodynamic data [5]; the reverse rate constants (R5, R6) are calculated from the forward rate constants through the equilibrium constants.

Table 2: Efficiency factors for third body term.

Ref. No	H	H ₂	H ₂ O	H ₂ O ₂	HO ₂	O	O ₂	OH
R5	1.0	2.5	12	1.0	1.0	1.0	1.0	1.0
R6	0.83	2.5	12	1.0	1.0	0.83	1.0	1.0
R7	0.75	2.5	12	1.0	1.0	0.75	1.0	1.0
R8	1.0	0.73	12	1.0	1.0	1.0	1.0	1.0
R9	1.0	2.5	12	1.0	1.0	1.0	1.0	1.0
R15	1.0	2.5	12	1.0	1.0	1.0	1.0	1.0

Table 3: Parameters of kinetic models and the computational costs. Case 1 — test case “ignition”, 38 cells; case 2 — test case “flame propagation”, 400 cells.

Model	Number of equations*	Number of species	Case 1, CPU hours/ms	Case 2, CPU hours/ms
Marinov <i>et al.</i> [23]	1	3 (H ₂ , O ₂ , H ₂ O) + N ₂	0.18	0.14
Lee and Kim [31]	2	4 (3 + H) + bath gas	0.43	0.20
abridged Jachimowski’s [22]	7	6 (3 + H, O, OH) + bath gas	1.7	5.2
Zhukov (this work)	13	8 + bath gas	1.6	19
Gutheil <i>et al.</i> [12]	21	8 + bath gas	2.5	67
O’Connaire <i>et al.</i> [15]	23	8 + bath gas	1.8	71
Konnov [14]	29	8 + bath gases	2.3	36
Burke <i>et al.</i> [16]	22	8 + bath gases	1.8	35

*) The number of equations could exceed the number of reactions because of the possible presence of double reactions and of third-body reactions where the activation energy depends on the collisional partner.

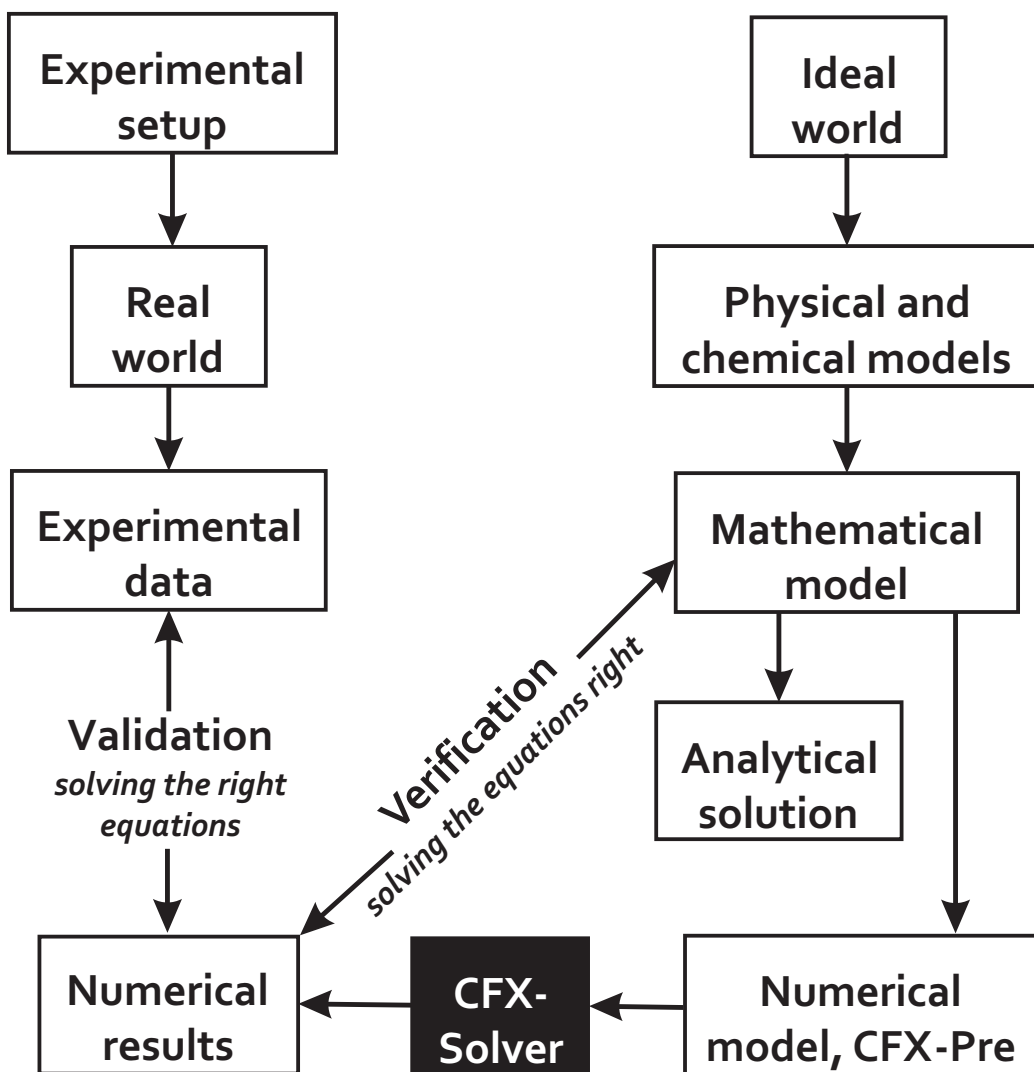


Figure 1: Logic scheme of validation and verification.

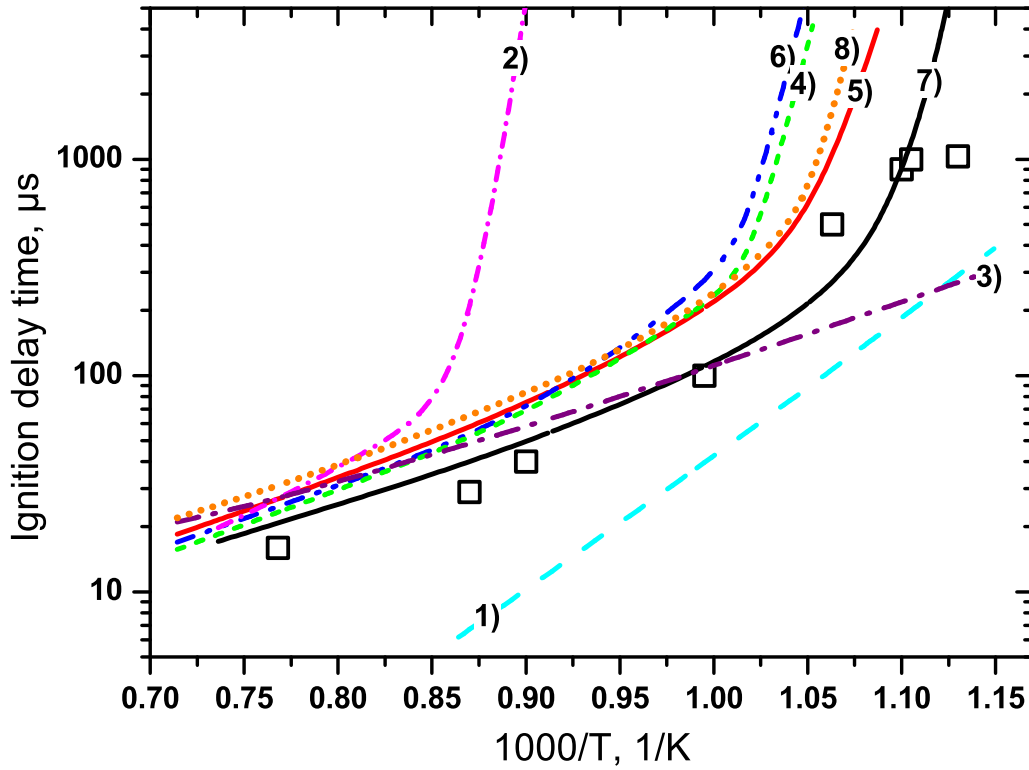


Figure 2: Ignition delay times of a stoichiometric hydrogen–air mixture at 1 atm. Squares — experimental data [25]; 1) dash cyan line — Marinov *et al.* [23]; 2) short dash dot magenta line — Lee and Kim [31]; 3) dash dot purple line — the abridged Jachimowski’s model [22]; 4) short dash line green — Zhukov (this work); 5) solid red line — O’Conaire *et al.* [15]; 6) dash dot dot line blue — Gutheil *et al.* [12]; 7) solid black line (the closest to exp. data) — Konnov [14]; 8) short dot orange line — Burke *et al.* [16].

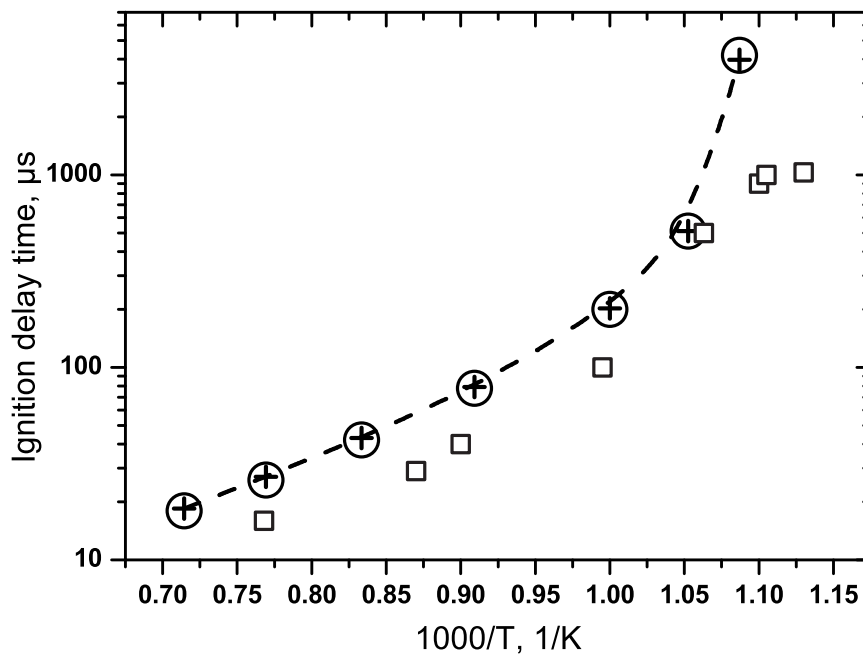


Figure 3: Comparison of the simulating data obtained using ANSYS CFX and CHEMKIN. Squares — the experimental ignition delay times of a stoichiometric hydrogen–air mixture at 1 atm [25]; the kinetic model by O’Conaire *et al.* [15]: dash line (B-spline) and crosses — ANSYS CFX, big circles — CHEMKIN.

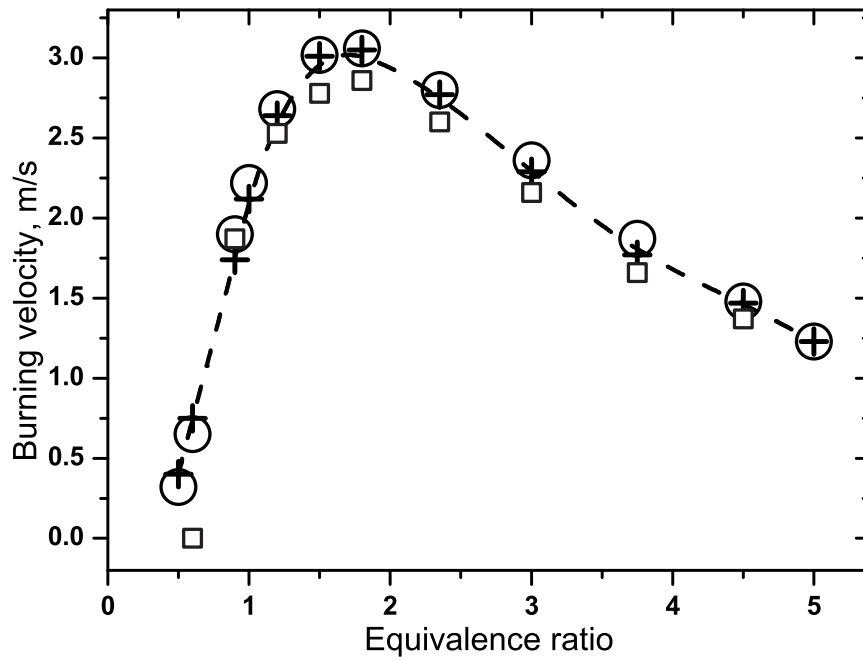


Figure 4: Comparison of the simulating data obtained using ANSYS CFX and CHEMKIN. Squares — the experimental burning velocities of a hydrogen–air mixture at 1 atm and 298 K [26]; the kinetic model by Konnov [14]: dash line (B-spline) and crosses — ANSYS CFX, big circles — CHEMKIN.

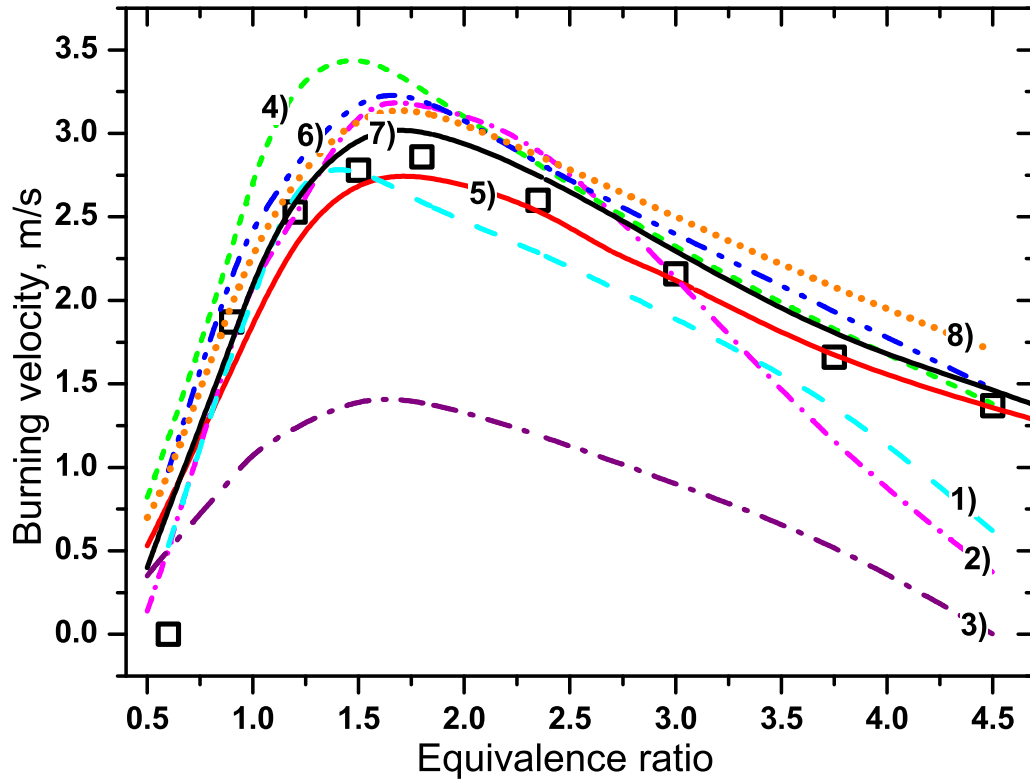


Figure 5: Burning velocities of a hydrogen–air mixture at 1 atm. Squares experimental data [26]; 1) dash cyan line — Marinov *et al.* [23]; 2) short dash dot magenta line — Lee and Kim [31]; 3) dash dot purple line — the abridged Jachimowski’s model [22]; 4) short dash line green — Zhukov (this work); 5) solid red line — O’Conaire *et al.* [15]; 6) dash dot dot line blue — Gutheil *et al.* [12]; 7) solid black line (the closest to exp. data) — Konnov [14]; 8) short dot orange line — Burke *et al.* [16].

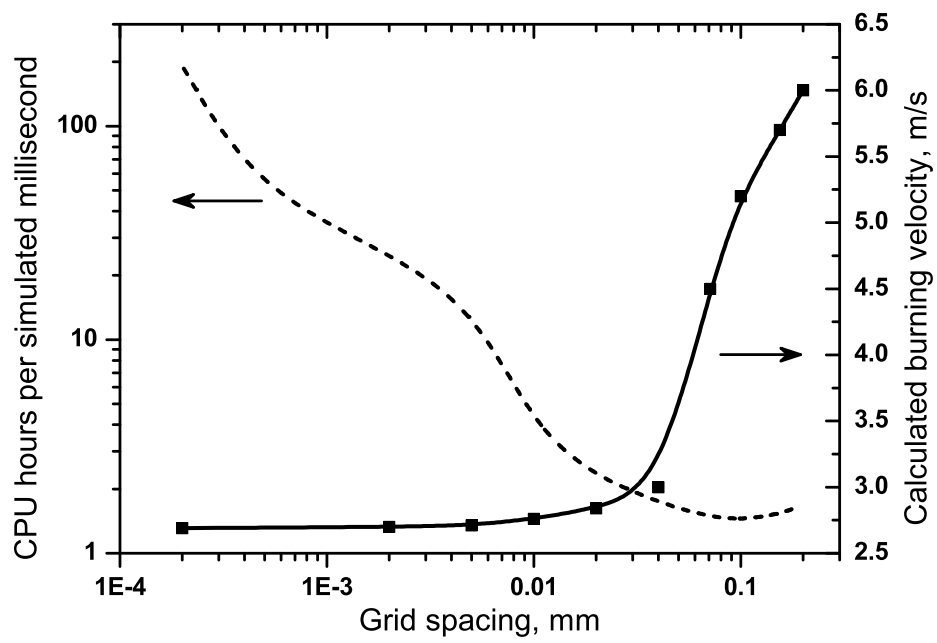


Figure 6: Simulating results and computational cost as the function of grid spacing. A hydrogen–air mixture at 1 atm, kinetic model by Zhukov (this work).